Mongolian Journal of Chemistry
www.mongoliajol.info/index.php/MJC

Influence of compressing pressure on macro void formation of carbon monolith for methane adsorption

B.Narandalai [1,2]*, W.G.Shim[2], M.S.Balathanigaimani[3], H.Moon[2]

[1]*Institute of Chemistry and Chemical Technology, Mongolian Academy of Sciences, MAS 4th building, Peace Avenue, Bayanzurkh district, Ulaanbaatar 13330, Mongolia*
[2]*Department of Advanced Chemicals & Center for Functional Nano Fine Chemicals Chonnam National University, Gwangju, Korea 61186*
[3] *Department of Chemical Engineering, Rajiv Gandhi Institute of Petroleum Technology, Ratapur Chowk, Rae Bareli, 229316 Uttar Pradesh, India*

*Corresponding author: naran.d10@gmail.com

Received: 28 September 2017; revised: 18 December 2017; accepted: 20 December 2017

ABSTRACT
Carbon monoliths for adsorbed natural gas (ANG) storage were prepared from Mongolian anthracite-based activated carbons using carboxy-methyl cellulose as a binder under different compressing pressures. Nitrogen adsorption/desorption experiments were carried out to obtain the specific surface area, pore volume, and pore size distribution of the monoliths. Methane adsorption experiments on the carbon monoliths were conducted at different temperatures and pressures up to around 3.5 MPa in a high pressure volumetric adsorption apparatus. As expected, adsorption results indicated that the methane adsorption capacity of the carbon monoliths increased with increasing specific surface area and packing density. The maximum volumetric adsorption of methane was observed as 163 V/V at 293 K and 3.5 MPa on a carbon monolith sample, PMAC1/2-3-65, that does not have the highest specific surface area but relatively high packing density comparing with other monoliths, which implies that two physical properties contribute contradictorily to the methane adsorption capacity. Based on experimental results, the carbon monoliths prepared from Mongolian anthracite-based activated carbons can be promising media for ANG storage application.

Keywords: Anthracite based activated carbons, carbon monoliths, methane adsorption, porous texture characterization, adsorbed natural gas storage

INTRODUCTION
The ANG has been known as a modern technology in which natural gas is adsorbed by porous materials at relatively low pressures around 3.5 MPa and at room temperature. Once a good medium with sufficient working capacity is developed, ANG will be competitive technically and economically comparing with the conventional storage methods such as LNG and CNG. In order to make this ANG as a competitive commercial technology, the DOE had set a storage target of 180 V/V at 3.5 MPa and 298 K in 2000 and modified this target up to more than 220 V/V that is the maximum achievable capacity based on carbon-based materials [1, 2]. Volumetric storage capacities for methane (a major constituent of natural gas) have been reported in the range from 150 to 200 V/V from bench-scale experiments but there is no information regarding the practical application of ANG technology. Methane adsorption on carbon materials has a rich history. ACs are excellent adsorbent materials for methane storage and expected to possess high surface area and proper pore size distribution. The ACs have been produced from various natural carbon materials [3]. However, the ACs produced from biomasses generally have low packing density and cannot achieve high ANG volumetric capacity, since the volumetric storage capacity is usually based not only on specific surface area but also on packing density of the adsorbent [4]. MRA, which is highly rich in carbon content, was used for preparing adsorbent material for specific applications such as gas and energy storages. The selection of MRA as a carbon source was due to less ash content, no need of carbonization step, high bulk density, and strong physical strength. It is a fossil fuel which has been formed at high temperature and pressure conditions during cluster movement. Hence it has intrinsically strong physical strength as well as high density, which could be effective in ANG application [5].
It would be of worth to make proper monoliths from powdered activated carbon with increased packing density. In general, the monoliths offer the increase in density by reducing the excess void volume, compactness and easy handling. Usually, the carbon monolith has been made by compressing a mixture of powdered activated carbon and binder. Several binders

have been used for making monoliths for this purpose [6]. In this study, the carbon monoliths were produced from the MRA-based activated carbons using CMC as a binder and assessed as storage materials for ANG technology. The effects of binder contents and compressing pressure for the preparation of carbon monoliths were also studied to understand how these properties would affect the formation of monoliths.

EXPERIMENTAL

Preparation of carbon monoliths: Activated carbon precursor - raw anthracite was supplied by Ikh gobi energy mine, East gobi province of Mongolia. The raw anthracite was powdered and sieved to get the powder with the particle size less than 53 μm.

Activated carbons were prepared from the MRA by varying the mass ratio of carbon precursor to activation agent from 2/1 to 1/4 according to the preparation method used in our previous work [7]. The activation agent was the KOH and it was physically mixed with powdered MRA prior to activation. Coin-type carbon monoliths for ANG application were fabricated from the PMAC series carbon powders using CMC as a binder. In fabricating the carbon monoliths, different binder contents (3, 5, and 10 wt.%) and compressing pressures (10, 25, 45, 55 and 65 MPa) were employed in order to elucidate the effect of preparation conditions on physical characteristics of the carbon monoliths. The corresponding amounts of activated carbon and binder were first thoroughly mixed in water and then the water present in the slurry was removed by heating. Finally, the resultant mixture was compressed at room temperature to make coin-type monoliths, followed by the complete drying in an oven for overnight at 378 K. The thickness and diameter of prepared monoliths were 5 - 6 mm and 31.5 mm, respectively.

The packing density of all prepared carbon monoliths was measured in terms of carbon precursor, compressing pressure and binder content to find reliable conditions for fabricating carbon monoliths systematically. In the sample naming, PMAC represents the MRA-based activated carbon prepared by chemical activation using potassium hydroxide as the chemical agent and the fractional number after PMAC does the mass ratio of MRA/agent in activation, as namely PMAC1/2. Other two numbers mean the binder content in weight percent and the compressing pressure in MPa, respectively. For example, PMAC1/2-3-65 sample represents the activated carbon prepared with mass ratio of ½ as the anthracite to potassium hydroxide, so then prepared activated carbon shaped with binder percent of 3 and compressing under pressure of 65 MPa.

Porous texture characterization: The porous textures of the prepared carbon monoliths were characterized using nitrogen adsorption and desorption isotherm data measured at 77 K (Micromeritics ASAP 2020, USA). Prior to the adsorption analysis, the sample was outgassed at 423 K for 12 h under vacuum condition for the removal of moisture and other impurities. The specific surface area was determined on the basis of the BET equation [8] using the relative nitrogen pressures (P/P_0) in the range of 0.01-0.05 as suggested by Kaneko *et al*. [9]. The pore size distribution, pore volume, and average pore width were also obtained by employing the DFT. Furthermore, the BJH [10] and the H-K equations [11] were used for the calculation of mesopore and micropore volumes, respectively. The APW was calculated by 4V/A using the BET results [12].

Adsorption equilibrium experiment: The major constituent of natural gas as a methane percent up to 90%, which was used for evaluating the adsorption capacity of prepared carbon monoliths. The adsorption of methane was carried out in a volumetric adsorption apparatus at three different temperatures (293.15, 303.15 and 313.15 K) and at pressures up to 3.5 MPa. The detailed description about operating procedures, volumetric adsorption apparatus, and schematic view of adsorption set-up are available in elsewhere [13].

RESULTS AND DISCUSSION

Characterization of Mongolian raw anthracite (MRA): In this study were used anthracite – based ACs. This ACs precursor's proximate analyses shown in Table 1. Listed data of MRA measured under three different conditions such as air-dry, dry, and dry-ash free (DAF) bases. The ash contents in MRA for air-dry and dry conditions were 10.74 and 10.82 wt.%, respectively, which are considerably lower than other carbon precursors. It should be noted that the content of fixed carbon measured under the DAF condition is over 90 wt.%.

Packing density of carbon monoliths: All the packing densities obtained are listed in Table 2. Figure 1 shows the effect of compressing pressure on the packing density of carbon monoliths. Owing to high compressing

Table 1. Proximate analyses of MRA

Sample	Air dried basis (%)				Dry basis (%)			DAF (%)	
	Moisture	Volatile matter	Ash	Fixed carbon	Ash	Volatile matter	Fixed carbon	Volatile matter	Fixed carbon
MRA (East Gobi)	0.74	7.99	10.74	80.53	10.82	8.05	81.13	9.02	90.98

DAF: Dry ash free (MRA: determined in the General laboratory of geology in Mongolia.)

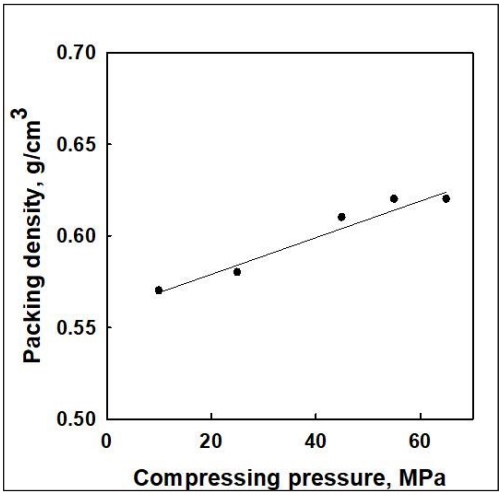

Fig. 1. Effect of compressing pressure on packing density density from monolith of PMAC1/2-3-65

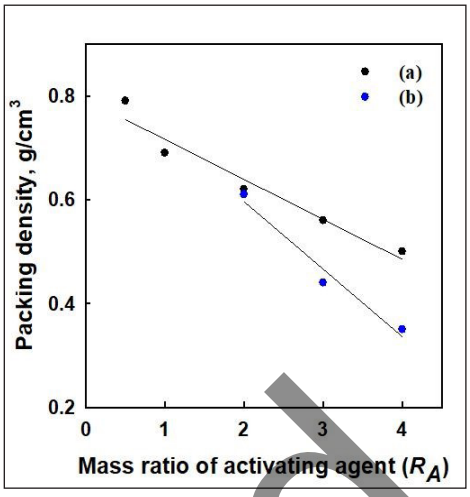

Fig. 2. Effect of R_A on packing density: (a) 65 MPa and 3 wt.% CMC, (b) 10 MPa and 10 wt.% CMC

pressures, the packing density of a series of carbon monolith was almost linearly increased from 0.56 to 0.62 g/cm^3. Their specific surface area (BET) was from 1115 to 1460 m^2/g, micropore volumes were from 0.54 to 0.65 cm^3/g, and mesopore volumes were from 0.14 to 0.29 cm^3/g, respectively.

The samples used here were the PMAC1/2-3-x series, which are activated with mass ratio of ½ as the anthracite to potassium hydroxide, so then obtained activated carbon powders shaped with binder percent of 3 and compressing under variable pressure (10, 25, 45, 55 and 65 MPa) for making carbon monolith.

This result implies that the compression destroys or reduces large internal pores inside the monolith and eventually its volume was reduced as expected.

The data in Figure 2 shows two experimental data sets of the packing density in terms of the mass ratio of agent/MRA (R_A) at the compressing pressures of 10 and 65 MPa, respectively. The binder content was fixed as 3 wt.% in these experiments. The packing density of carbon monoliths was decreased linearly with the mass of the activating agent that was used for activation. This result surely comes from the difference in particle density of original activated carbon samples that were produced with different mass of the activating agent. It has been already known that an activated carbon sample, which was prepared with higher mass ratio of activating agent, has higher specific surface area, higher pore volume, and lower particle density since more internal pores were formed during chemical activation [7]. Especially, when a low compressing pressure of 10 MPa was used, the decreasing slope of the packing density vs became steeper. This shows that the effect of compressing pressure on the packing density of carbon monoliths

Table 2. Effect of binder proportion and compression pressure on the physical properties and dimensions of carbon monoliths

Carbon monolith	Binder (CMC)	P_{comp}	Mass	Volume	Packing density
	(%)	(MPa)	(g)	(cm^3)	(g/cm^3)
PMAC 2/1-3-65	3	65	1.85	2.34	0.79
PMAC1/1-3-65	3	65	1.69	2.46	0.69
PMAC1/2-3-65	3	65	2.82	4.54	0.62
PMAC1/3-3-65	3	65	2.45	3.35	0.56
PMAC1/4-3-65	3	65	2.46	4.89	0.50
PMAC1/2-3-55	3	55	2.99	4.83	0.62
PMAC1/2-3-45	3	45	2.14	3.53	0.60
PMAC1/2-3-25	3	25	1.87	3.21	0.58
PMAC1/2-3-10	3	10	2.87	5.06	0.56
PMAC1/2-5-65	5	65	2.89	4.55	0.64
PMAC1/2-10-65	10	65	3.00	4.30	0.70
PMAC1/2-10-10	10	10	3.22	5.27	0.61
PMAC1/3-10-10	10	10	3.12	7.02	0.44
PMAC1/4-10-10	10	10	3.21	9.22	0.35

may be larger at lower compressing pressures. Figure 3 shows the effect of binder content on the packing density of carbon monoliths. The packing density increases with the binder content. The sum of micropore- and mesopore volumes is also shown in Figure 3 in order to compare with the variation of the packing density.

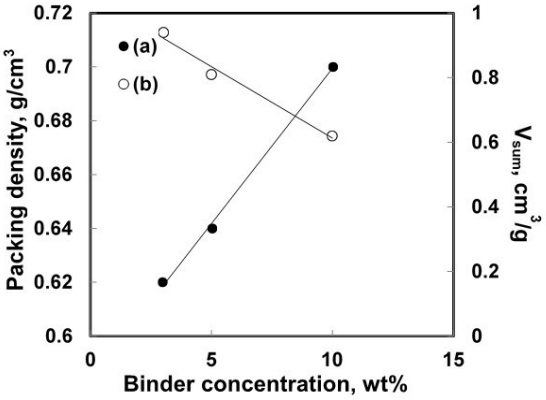

Fig. 3. Effect of binder concentration on the packing density (●) and total pore volumes, V_{SUM} (○) from monolith of PMAC1/2-3-65

This result seems to be closely related with the penetration of binder into internal pores of carbon monoliths by compression for fabricate which implies a reduction of porosity due to partial blocking, the extent of which depends on the kind and proportion of binder used [14].

In general, the packing density is a major working parameter to develop adsorption media for energy storages because the volumetric capacity is much more important than the gravimetric one.

It is to be noted that activated carbons with highly developed pores are not always good media for storing any gas such as methane, which has been used as a fuel for moving vehicles [15]. Low packing density can cause the decrease in volumetric capacity considerably, adsorption capacity by well-developed surface area. Therefore it can be proposed that there may be an optimum in fabricating carbon monoliths for methane storage.

Textual properties of carbon monoliths: Figure 4 shows the adsorption isotherms of nitrogen, the adsorbed volume of nitrogen in cm^3/g at 298 K and 0.1 MPa (STP) in terms of partial pressure, measured at 77K. All the isotherms show typical three steps in terms of relative pressure such as a very steeply increasing sector without hysteresis at low relative pressures, a slowly increasing one with notable hysteresis, and a final abrupt saturation, which show volume filling in small micropores, progressive filling of large micropores and mesopores, and active capillary condensation at near the saturation pressure of nitrogen, respectively [9]. In the case of effect of mass ratio of anthracite/KOH for preparing ACs on carbon monolith (Figure 4(a)), three monoliths fabricated from the activated carbon.

PMAC1/4 (R_A= 4), have the Type II isotherm whereas the others (PMAC1/2-10-10 and PMAC1/3-10-10) do

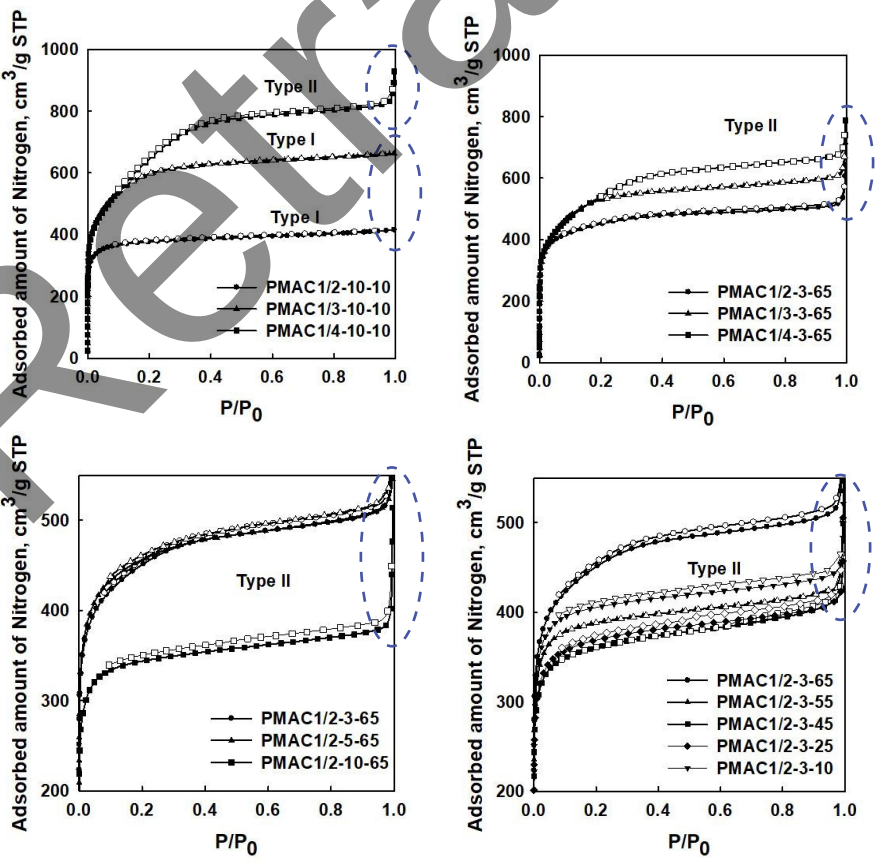

Fig. 4. Nitrogen adsorption/desorption isotherms of PMAC-series monoliths,
(a) and (b) in terms of mass ratio (R_A),(c) in terms of binder content, (d) in terms of compressing pressure

Table 3. Textural properties of carbon monoliths

Carbon monoliths	S_{BET}	Pore volumes (cm^3/g)			Pore width (nm)		
	m^2/g	V_{HK}	V_{BJH}	V_{total}	D_{HK}	D_{BJH}	D_{APW}
PMAC2/1-C3-65	622	0.30	0.10	0.40	0.49	3.15	2.57
PMAC1/1-C3-65	845	0.41	0.14	0.55	0.51	3.18	2.60
PMAC1/2-C3-65	1460	0.65	0.29	0.94	0.54	2.49	2.35
PMAC1/3-C3-65	1757	0.74	0.23	0.97	0.60	3.57	2.30
PMAC1/4-C3-65	1854	0.73	0.45	1.18	0.58	2.93	2.40
PMAC1/2-C3-55	1219	0.58	0.16	0.74	0.58	3.29	2.43
PMAC1/2-C3-45	1115	0.54	0.18	0.72	0.54	3.32	2.39
PMAC1/2-C3-25	1170	0.55	0.18	0.73	0.49	2.99	2.35
PMAC1/2-C3-10	1249	0.61	0.14	0.75	0.53	2.88	2.33
PMAC1/2-C5-65	1443	0.67	0.27	0.94	0.53	2.54	2.19
PMAC1/2-C10-65	1056	0.51	0.15	0.66	0.49	2.75	2.26
PMAC1/2-C10-10	1174	0.57	0.11	0.68	0.51	2.83	2.09
PMAC1/3-C10-10	1975	0.82	0.45	1.27	0.56	2.21	2.04
PMAC1/4-C10-10	2299	0.83	1.04	1.87	0.59	2.29	2.26

S_{BET} - BET specific surface area, V_{total} - sum of the HK and BJH pore volume, V_{HK} - micropore volume, determined using the HK method, V_{BJH} - mesopore volume, determined using the BJH method, D_{APW}- average pore width, calculated by 4 V_t/S_{BET} using BET.

have the Type I according to the IUPAC classification [7]. Such results come from the pore structure of the original activated carbon rather than monoliths themselves. First two diagrams (a) and (b) in Figure 4 show the effect of R_A on nitrogen adsorption capacity on the monoliths fabricated with two different compressing pressures, 10 and 65 MPa, respectively. The binder content was fixed as 10 and 3 wt.%. When a monolith was made from activated carbon prepared using higher R_A, it had higher gravimetric adsorption capacities because of well-developed pore structure with large specific surface area. The effect of R_A on the gravimetric adsorption capacity appears greater when lower compressing pressure was employed. The textural properties of the monoliths such as the BET surface area, pore volumes, and pore width were calculated from nitrogen adsorption/desorption data and listed in Table 3. The HK [11] and BJH [10] methods were employed for calculating micropore and mesopore volumes, V_{HK} and V_{BJH}, respectively. From Table 3, it is possible to withdraw several important results for future discussion. Firstly it is noted that S_{BET}, V_{HK} and V_{BJH} of carbon monoliths increased monotonously with the amount of activating agent used in the chemical activation for original activated carbons, namely R_A. When a binder content of 3 wt.% was used and the compressing pressure was 65 MPa, the BET specific surface area increase from 622 to 1854 m^2/g in the range of R_A= 0.5 ~ 4. Under the same conditions, the sum of V_{HK} and V_{BJH} (V_{total}) increased from 0.40 to 1.18 cm^3/g. The same results were also obtained for the carbon monoliths fabricated under a compressing pressure of 10 MPa, as shown in the last three rows in Table 3. Secondly, it is interesting to see the effect of compressing pressure on the textual properties of carbon monoliths.

When the compressing pressure was increased from 10 to 65 MPa, S_{BET} and V_{total} of the carbon monoliths show unexpected results; they were slightly decreased up to 45 MPa but steeply increased after 55 MPa over the values obtained at 10 MPa. It is not easy to interpret such a peculiar result based on the concept of simple compression. It is also contradictory with the variation of packing density in terms of compressing pressure, mentioned in the previous section 3.1 since the packing density is generally inversely proportional with the pore volume. However, one can postulate the SDP by means of increasing compressing pressure. Most carbon monoliths have considerable number of macropores, of which textual properties cannot be measured from nitrogen adsorption/desorption data. According to the increase in compressing pressure, macropores would be destroyed producing mesopores and the destruction of some mesopores coincides forming micropores in Figure 5.

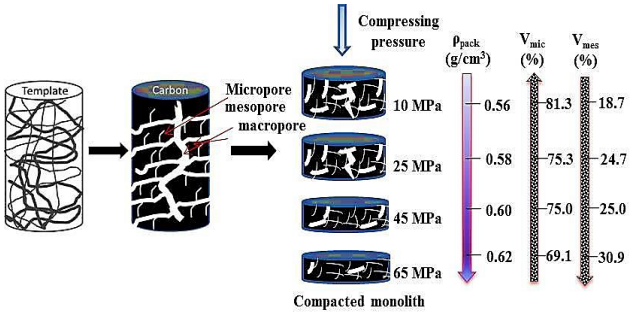

Fig. 5. Schematic diagram of the preparation of AC monolith

Over a critical compressing pressure, such SDP occur entirely inside the carbon monolith and many micropores and mesopores can be formed, eventually S_{BET} and V_{total} are increased considerably. This SPD concept cannot be explained all experimental results which are related with the textual properties, for example the slight decrease in V_{HK} at 25 and 45 MPa, but it can give a clue for considerable increase in such properties over 55 MPa. This deduction can be confirmed directly from the SEM images of the carbon monoliths fabricated at 10, 45 and 65 MPa, showing sizeable decrease in grain diameter and inter-grain width (shown in Figure 6).

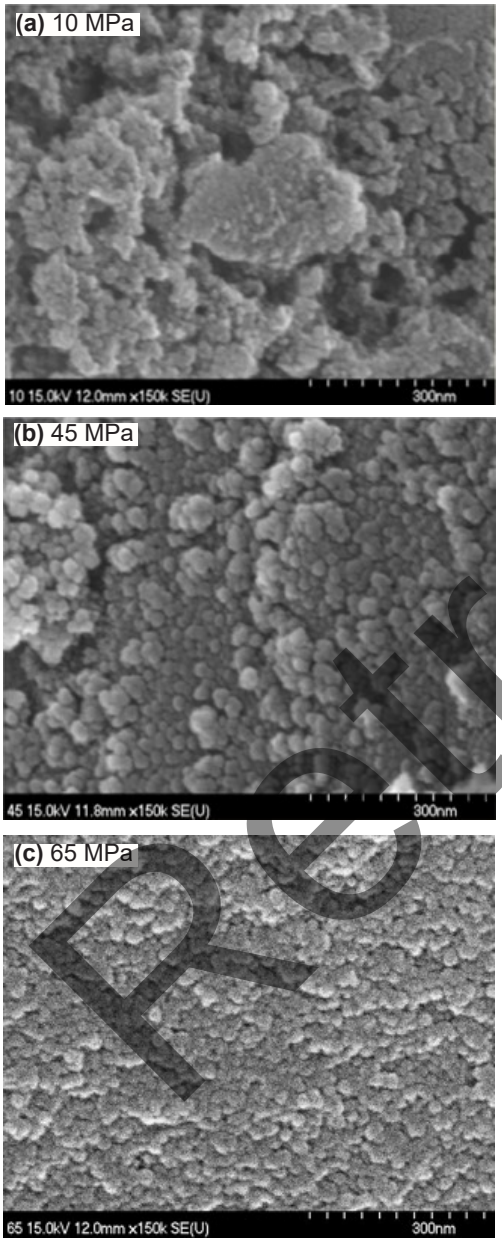

Fig. 6.The SEM images with compressing pressure

Finally, it is worth noting that the use of binder has adverse effects on all the textual properties of carbon monoliths except the enhancement of physical strength. This is the reason behind minimized the amount of binder for best one which may guarantee its physical strength for use.

PSDs and AEDs: The pore size distribution of a medium has been known as very important information in most storage applications such as the ANG and the EDLC since it influences the adsorption capacity and the mobility of gas molecules and ions inside the medium. The PSDs calculated from the DFT are shown in Figure 7 for two sets of carbon monoliths compressed at 10 and 65 MPa. In the case of a relatively low compressing pressure of 10 MPa, it is shown that large micropores and small mesopores were developed well, especially in the carbon monoliths that were activated with high R_A (see PMAC1/4-10-10).

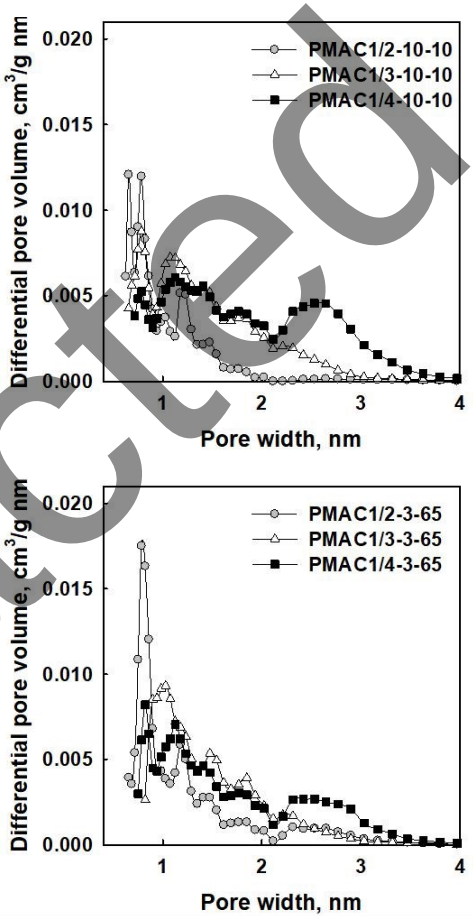

Fig. 7. Pore size distributions of PMAC1/x-10-10 and PMAC1/x-3-65 series monoliths in terms of mass ratio

When the compressing pressure was increased to 65 MPa, small mesopores in the range of 2 ~ 4 nm were destructed considerably. Such a result could be expected from the results mentioned in the previous section. The most interesting result was found in the case of PMAC1/2-3-65, which showed the notable formation of micropores less than 1 nm and mesopores around 2 nm. This seems to be a critical clue for the SDP during compression under high compressing pressures. Furthermore, it is notable that most carbon monoliths have well-developed micropores in the range from 0.8 to 2 nm, which has been known as a proper range of pore sizes for methane storage application. The van der Waals diameter of methane molecule is 0.43 nm.

The energetic heterogeneity properties of carbon

materials have been characterized using their AEDs. All AEDs for carbon monoliths used in this work were calculated from nitrogen adsorption data using the Fowler-Guggenheim equation as an energy dependent local isotherm [18]. The distribution function, *F(U)*, is given as follows:

$$\theta(\mathrm{P}) = \int_{\Delta} \theta_1(P,U)F(U)dU \quad \textbf{(1)}$$

where:

θ(P) - sub-monolayer surface coverage

$\theta_1(P, U)$ - energy dependent local adsorption isotherm

F(U)dU - denotes the fraction of the surface with adsorption energies between *U* and *U+dU*

The AEDs for the same sets of carbon monoliths depicted in Figure 7 are shown in Figure 8 for comparative discussion. In general, the AED with two peaks indicates that the prepared carbon monolith has two distinct pore structures, namely micropores and mesopores.

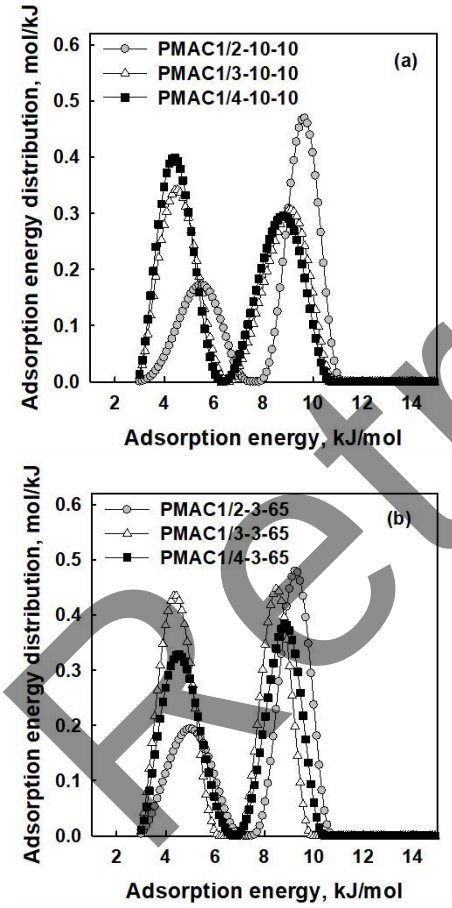

Fig. 8. AEDs of PMAC1/x-10-10 and PMAC1/x-3-65 series monoliths in terms of mass ratio

The AED can be characterized by the location, width and height of each peak. Usually the peak with higher adsorption energy has been known to be related with small micropores and vice versa. In this analysis the adsorption energy itself could be considered as a relative index rather than a decisive one. The peak width can be a criterion for surface heterogeneity. A narrower AED represents the smaller energetic surface heterogeneity. From the peak height, one can estimate the portion of pores with a range of size that stands for the location of corresponding adsorption energy.

Based on the discussion above, several significant results can be drawn from the AEDs in Figure 8. As expected from the pore size distributions for the PMAC1/4 series in Figure 7, the peak height at higher adsorption energy increased while that at lower adsorption energy decreased considerably when the carbon monolith was compressed under a high pressure of 65 MPa. This result implies the destruction of mesopores and the formation of micropores during compression. However, two AED peaks for the PMAC1/3 series compressed at 65 MPa were increased simultaneously compared with those at 10 MPa, which indicates the formation of two distinct pores at the same time. This fact was not found evidently from the PSDs given in Figure 7. In the case of the PMAC1/2 series, it was confirmed that the peak at lower adsorption energy became larger and wider at 65 MPa, showing the formation of mesopores having various sizes whereas the peak at high adsorption energy remained without any specific change which is not expected from its corresponding PSD with considerable increase in micropore ranges. Conclusively the results obtained from PSD and AED for a given medium can confirm each other and show complementary cooperation in analyzing the pore structure of the medium.

Adsorption equilibrium of methane on carbon monoliths: Methane adsorption capacities of carbon monoliths were measured at 293 K and at pressures up to 3.5 MPa. The gravimetric adsorption amounts of methane on two carbon monolith series are shown in Figure 9 to investigate the effects of binder content and compressing pressure on the methane adsorption capacity of carbon monoliths. When the binder content was increased from 3 to 10 wt.%, the adsorption capacity was decreased considerably due to pore blocking by the penetration of binder into the internal pores of carbon monoliths. The adsorption equilibrium of methane on the carbon monoliths were described using the Sips isotherm model with three adjustable parameters:

$$q = \frac{q_m b P^{1/n}}{1 + b P^{1/n}} \quad \textbf{(2)}$$

where:

q_m - maximum adsorption capacity

All isotherm parameters were determined from the fitting of experimental equilibrium data with the Sips model. The parameters for the equilibrium data sets depicted in Figure 9(a) are listed as well as the SOR for comparison in Table 4. The SOR value for each experimental data set was obtained by the following equation:

$$\mathrm{SOR} = \frac{1}{n}\sum_{i=1}^{n}\left(q_i^{exp} - q_i^{cal}\right)^2 \quad \textbf{(3)}$$

where:

q^{exp} - experimental adsorbed amount

q^{cal} - calculated adsorbed amount [19]

Table 4. Sips isotherm parameters for methane adsorption on carbon monoliths of PMAC1/2-x-65

Adsorbent	Temperature	q_m	b	n	SOR
	K	mmol g^{-1}	bar^{-n}		
PMAC1/2-3-65	293.15	21.5	0.048	0.858	0.005
PMAC1/2-5-65	293.15	14.3	0.094	0.763	0.240
PMAC1/2-10-65	293.15	9.32	0.133	0.775	0.011
PMAC1/2-3-65	303.15	19.0	0.05	0.835	0.013
PMAC1/2-3-65	313.15	18.9	0.04	0.806	0.048

Adsorption isotherms of methane on the carbon monoliths that were fabricated under various compressing pressures from 10 to 65 MPa are shown in Figure 9(b). Two significant results were withdrawn from these isotherms.

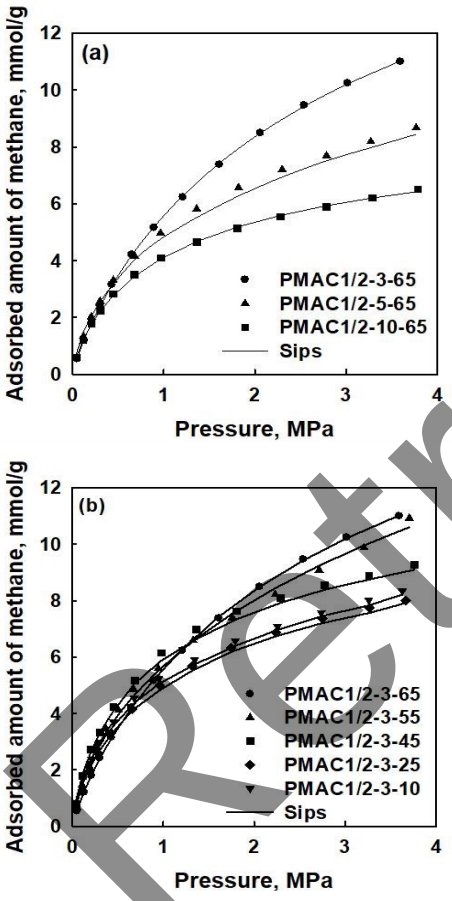

Fig. 9. Adsorbed amount of methane on PMAC1/2-series monoliths (a) in terms of binder content, (b) in terms of compressing pressure

Firstly, the carbon monolith compressed at the highest pressure of 65 MPa had the highest gravimetric adsorption capacity of methane at the target pressure of 3.5 MPa. It was very unfortunate that any larger pressure over 65 MPa could not be used in compressing carbon monoliths due to the limit of our compressing unit. As expected from the pore volumes and PSDs obtained from nitrogen adsorption data in the previous sections, the gravimetric adsorption capacity of methane was first decreased slightly but increased gradually with the compressing pressure. Secondly the variation in the initial slope of adsorption isotherms has significant meaning for ANG. The isotherms obtained on the carbon monoliths compressed at low pressures had steep slopes at low relative pressures but these slopes were gradually reduced with the compressing pressure. It seems to be a very desirable character for ANG storage application. For the purpose to isolate any target gas like that in environmental remediation, the steep slope of its isotherm at low relative pressures is quite desirable. However, in the case of any cyclic operation that consists of repeated adsorption and desorption steps, such a condition can reduce the working capacity greatly.

Adsorption isotherms of methane on PMAC1/2-3-65 were also measured at three different temperatures of 293, 303, and 313 K and shown in Figure 10. In overall, the adsorption amount of methane decreased with temperature, which indicates that the adsorption of methane on carbon monoliths was mainly physical

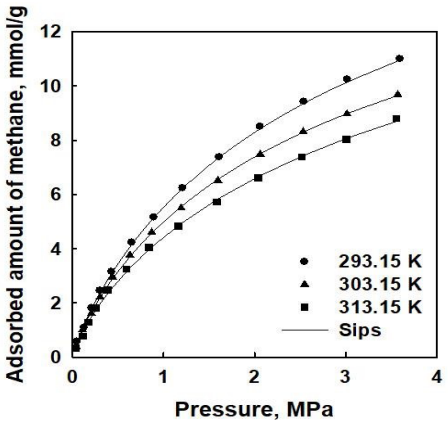

Fig. 10. Adsorbed amount of methane in terms temperature (PMAC1/2-3-65)

rather than chemical. The Sips isotherm parameters were also calculated and listed in Table 4.

Volumetric storage capacity of methane: For ANG storages, the volumetric capacity for methane must be determined especially when ANG are to be used as fuel for vehicles. The volumetric adsorption capacity per a unit volume of storage vessel (V/V) is generally calculated using the gravimetric adsorption amount per a unit mass of medium (Q) and the packing density of carbon monoliths using the following equation [20]:

$$V/V = QM\nu\rho_{pack} \quad (4)$$

where:

M - molecular weight of the target gas

v - volume occupied by 1 g of methane in the STP condition, which is 1.5 dm^3/g,

ρ_{pack} - packing density of the adsorbent.

The gravimetric storage capacity, *Q*, can be obtained from the changes in pressure in the loading and adsorption cells before and after adsorption equilibrium experiments in a high pressure adsorption unit using the following equation:

$$\left.\frac{PV}{ZRT}\right|_{L1} + \left.\frac{PV}{ZRT}\right|_{A1} = \left.\frac{PV}{ZRT}\right|_{L2} \left.\frac{PV}{ZRT}\right|_{A2} + QM \quad (5)$$

where:

P - pressure

T - temperature

V - volume

R - universal gas constant

M - mass of adsorbent

Z - compressibility factor.

The subscripts *L* and *A* represent a loading cell and an adsorption cell, respectively. The states before and after adsorption are indicated by numeric subscripts 1 and 2 [19, 21-27], respectively. All gravimetric and volumetric storage capacities for methane of the carbon monoliths used were obtained at 293 K and 3.5 MPa and listed in Table 5. The maximum gravimetric capacity for methane storage was 12.1 mmol/g using PMAC1/4-3-65 whereas the volumetric one was 163.6 V/V using PMAC1/2-3-65. At first, the effect of binder content on the gravimetric and volumetric storage capacity for methane was investigated. When the binder content was increased from 3 to 10 wt.%, the gravimetric capacities of the PMAC1/2 series carbon monoliths were decreased from 10.9 to 6.51 mmol/g while the volumetric capacities from 163.6 to 106.8 V/V. Therefore, considering the guarantee of mechanical strength, the binder content was fixed as 3 wt.% afterward.

Table 5. Methane adsorption capacity of carbon monoliths

Carbon monolith	Adsorption capacity at 293.15 K and 35 bar	
	Q (mmol/g)	V/V (cm^3/cm^3)
PMAC2/1-3-65	2.30	43.6
PMAC1/1-3-65	3.63	60.1
PMAC1/2-3-65	10.9	163
PMAC1/3-3-65	11.0	148
PMAC1/4-3-65	12.1	145
PMAC1/2-3-55	9.95	142
PMAC1/2-3-45	9.25	133
PMAC1/2-3-25	8.02	112
PMAC1/2-3-10	8.21	110
PMAC1/2-5-65	8.66	133
PMAC1/2-10-65	6.51	109
PMAC1/2-10-10	8.44	124
PMAC1/3-10-10	11.0	116
PMAC1/4-10-10	12.5	105

In analyzing the storage capacities for methane of carbon monoliths, one of major parameters is the mass ratio of activating agent (R_A) that was used during activation to make the original activated carbon. When R_A was changed from 0.5 to 4 (PMAC-2/1-3-10 PMAC-1/4-3-10), the volumetric storage capacity was varied from 43.4 to 163. 6 V/V. These results are shown in Figure 11 to find an optimum R_A in activating Mongolian anthracite. As mentioned in the previous section 3.1, when a high R_A was used, the activated carbon obtained had large BET specific surface area and pore volume and then it had eventually high gravimetric storage capacity for nitrogen or methane as shown in Tables 3 and 5. However the packing density was gradually decreased with R_A due to well-developed internal pores. From this contradictory effect there would be an optimum R_A in assessing the volumetric storage capacity of any medium. As shown in Figure 11, the maximum volumetric capacity for methane existed at around R_A = 2 when the binder content was 3 wt.% and the compressing pressure was 65 MPa.

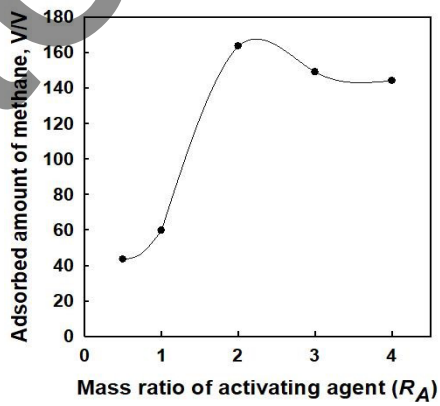

Fig. 11. Volume basis adsorbed amount of methane on PMAC2/1-3-65 ~ PMAC1/4-3-65 in terms of mass ratio of activating agent

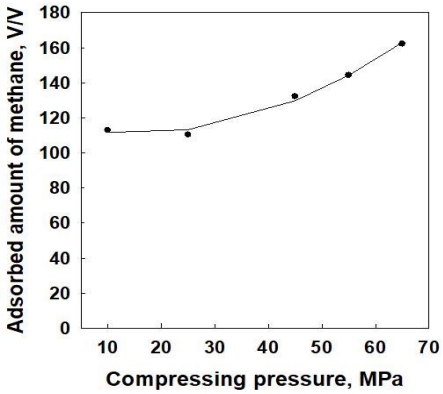

Fig. 12. Volume basis adsorbed amount of methane on PMAC1/2-3-65 in terms of compressing pressure

Table 6. Methane adsorption capacities of anthracite-based activated carbon monoliths (PMAC1/2-3-55) at 298.15K (examined 6 times)

Adsorption capacity	1	2	3	4	5	6	average
Mass basis, mmol/g	10.9	10.3	10.1	9.75	9.11	9.59	9.95
Volume basis, V/V	159	147	143	139	130	136	142

Figure 12 shows the variation of the volumetric storage capacity for methane in terms of compressing pressure when the binder content and R_A were fixed as 3 wt.% and 5, respectively. For this set of data, it was concluded that the storage capacity was gradually increased with the compressing pressure up to 65 MPa except a slight decrease at 25 MPa. This exceptional result is expected from the unusual variation in textual properties that has been discussed sufficiently in the section 3.2 based on a postulate of the SDP.

Finally, several adsorption/desorption experiments with the same carbon monolith were carried out to check the variation in the volumetric storage capacity during repeated use.

Figure 13 and Table 6 showed the variation of V/V during 6 cycles in a high pressure storage unit. The carbon monolith used was PMAC1/2-3-65. The storage capacity was gradually decreased from 163. 7 to 136.8 V/V after 6 repeated cycles. This result implies that the working capacity of such carbon monolith was about 84% of the original storage capacity. Such a decrease in the storage capacity usually depends on the

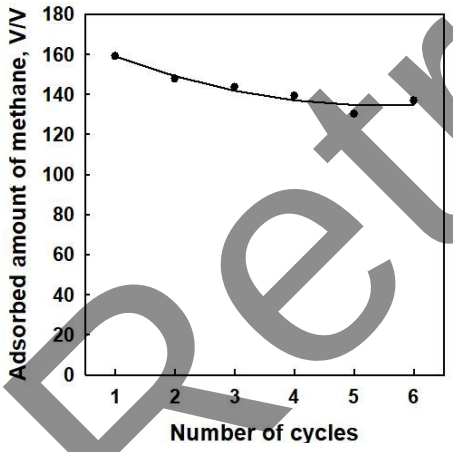

Fig. 13. Volume basis adsorbed amount of methane on PMAC1/2-3-55 in terms of number of cycles

irreversible adsorption amount at desorption pressure about 0.1 MPa since considerable amount of methane still remained in extremely small micropores and strong irreversible sites in the carbon monoliths. To obtain reliable working capacity of prepared carbon monoliths, a more detailed dynamic study is preferred.

CONCLUSIONS

In this paper extensively studied the Mongolian anthracite-based activated carbon monoliths were prepared under various compressing pressures, and the effects of mass ratio of activating agent, binder content on the packing density for the methane storage capacity. The packing density increased almost linearly with the compressing pressure while it linearly decreased with the mass of the activating agent that was used for activation. The texture properties such as BET specific surface area and total pore volumes determined from nitrogen adsorption data gradually decreased up to the compressing pressure of 45 MPa but steeply increased after 65 MPa over the values obtained at 10 MPa,1115 –1460 m^2/g, 0.72-0.94 cm^3/g. According to the increase in compressing pressure, macropores would be destroyed producing mesopores and the destruction of some mesopores coincides forming micropores. Over a critical compressing pressure (45 MPa), such SDP occur entirely inside the carbon monolith and many micropores and mesopores can be formed, eventually S_{BET} and V_{total} are increased considerably. This postulate was further confirmed by pore size distributions and adsorption energy distributions. The adsorption equilibrium of methane on carbon monoliths can be fitted well with the Sips isotherm and is physical rather than chemical. The volumetric storage capacity was increased with the compressing pressure with a slight decrease at 25 MPa, which can be also explained by the SDP concept properly. It was also noted that the optimum mass ratio of activating agent was around 2 for methane storage. The maximum volumetric capacity of 163.7 V/V was attained at 293 K and 3.5MPa using PMAC1/2-3-65 and the working capacity after 6 repeated cycles becomes 84% of the original capacity. Based on all results obtained in this work, it is proposed that the carbon monoliths fabricated from Mongolian anthracite-based activated carbons can be a reliable candidate as storage media for ANG and other energy storage applications.

ACKNOWLEDGEMENTS

This research was supported by the Korea-India International Cooperation Program from the Ministry of Science, ICT and Future Planning, Republic of Korea (NRF-2012K1A3A1A19036491) and Department of Science and Technology (Sanction Order No: INT/KOREA/P-17). The authors gratefully acknowledge the Mineral Resources Authority of Mongolian government, officer of Coal division Myagmar Davaadorj for supplying Mongolian raw anthracite for this research work.

REFERENCES

1. Pupier O., Goetz V., Fiscal R. (2005) Effect of cycling operations on an adsorbed natural gas storage. *Chem. Eng. Process*, **44**, 71-79.
2. Starling K.E., Ding E.R., Harwell J.H., Mallinson R.G. (1995) Method for improving natural gas energy density at ambient temperatures. *Energ.*

Fuel, **9,** 1062-1065.
3. Saez A., Toledo M. (2009) Thermal effect of the adsorption heat on an adsorbed natural gas storage and transportation systems. *Appl. Therm. Eng.,* **29***,* 2617-2623.
4. Zhang T., Walawender W.P., Fan L.T. (2010) Grain-based activated carbons for natural gas storage. *Bioresour. Technol*., **101**, 1983-1991.
5. Lee H.C., Byamba-Ochir N., Shim W.G., Balathanigaimani M.S., Moon H. (2015) High–performance super capacitors based on activated anthracite with controlled porosity. *J. Power. Sources,* **275**, 668-674.
6. Rahman K.A., Loh W.S., Chakraborty A., Saha B.B., Chun W.G., Ng K.C. (2011) Thermal enhancement of charge and discharge cycles for adsorbed natural gas storage. *Appl. Therm. Eng.,* **31**, 1630-1639.
7. Narandalai B., Shim W.G., Balathanigaimani M.S., Moon H. (2016) Highly porous activated carbons prepared from carbon rich Mongolian anthracite by direct NaOH activation. *Appl. Surf. Sci.,* **379**, 331-7.
8. Branauer S., Emmett P.H., Teller E. (1939) Adsorption of gases in multimolecular layers. *J. Am. Chem. Soc.,* **60,** 309-19.
9. Kaneko K., Ishii C., Ruike M., Kuwabara H. (1992) Origin of superhigh surface area and microcrystalline graphitic structures of activated carbons. *Carbon,* **30***,* 1075-88.
10. Barret E.P., Joyner L.G., Halenda P.P. (1951) The determination of pore volume and area distribution in porous substances. I. Computations from nitrogen isotherms. *J. Am. Chem. Soc.,* **73**, 373-80.
11. Horvath G., Kawazoe K.J. (1983) Method for the calculation of effective pore size distribution in molecular sieve carbon. *Chem. Eng. Jpn.,* **16**, 470-5.
12. Giraldo L., Moreno-Pirajan J.C. (2011) Novel activated carbon monoliths for methane adsorption obtained from coffee husks. *Mater. Sci. Appl.,* **2**, 331-9.
13. Delavar M., Ghoreyshi A.A., Jahanshahi M., Irannejad M. (2010) Experimental evaluation of methane adsorption on granular activated carbon (GAC) and determination of model isotherm. *Int. J. Chem. Mol. Nucl. Mater. Metall. Eng.,* **4**,153-156.
14. Ramos-Fernandez J.M., Martinez-Escandell M., Rodriguez-Reinoso F. (2008) Production of binderless activated carbon monoliths by KOH activation of carbon mesophase materials. *Carbon,* **46**, 384-386.
15. Celzard A., Albiniak A., Jasienko-Halat M., Mareche J.F., Furdin G. (2005) Methane storage capacities and pore textures of active carbons undergoing mechanical densification. *Carbon,* **43**, 1990-1999.
16. Landers J., Gor G.Y., Neimark A.V. (2013) Density functional theory methods for characterization of porous materials. *Colloids Surf. A,* **437**, 3-32.
17. Lastoskie C., Gubbins K.E., Quirkeft N. (1993) Pore size distribution analysis of microporous carbons: a density functional theory approach. *Phys. Chem.,* **97**, 4786-4796.
18. Rudzinski W., Jaroniec M., Sokolowski S. (1975) Gas adsorption on heterogeneous surfaces: a detailed computation of adsorption energy distribution. *Czech. J. Phys. B,* **25**, 891-901.
19. Balathanigaimani M.S., Shim W.G., Lee M.J, Lee J.W., Moon H. (2008) Charge and discharge of methane on phenol-based carbon monolith. *Adsorption,* **14**, 525-532.
20. Celzard A., Perrin A., Albiniak A., Broniek E., Mareche J.F. (2007) The effect of wetting on pore texture and methane storage ability of NaOH activated anthracite. *Fuel,* **86**, 287-293.
21. Vargas D.P., Giraldo L., Moreno-Pirajan J.C. (2013) Carbon dioxide and methane adsorption at high pressure on activated carbon materials. *Adsorption,* **19**, 1075-1082.
22. Vargas D.P., Giraldo L., Moreno-Pirajan J.C. (2012) CO_2 adsorption on activated carbon honeycomb-monoliths: a comparison of Langmuir and Toth models. *Int. J. Mol. Sci.,* **13**, 8388-8397.
23. Guan C., Loo L.S., Wang K., Yang C. (2011) Methane storage in carbon pellets prepared via a binderless method. *Energy. Convers. Manage,* **52**, 1258-1262.
24. Yeon S.H., Knoke I., Gogotsi Y., Fischer J.E. (2010) Enhanced volumetric hydrogen and methane storage capacity of monolithic carbide-derived carbon. *Micropor. Mesopor. Mater.,* **131**, 423-8.
25. Fan S., Yang L., Wang Y., Lang X., *et al*. (2014) Rapid and high capacity methane storage in clathrate hydrates using surfactant dry solution. *Chem. Eng. Sci.,* **106**, 53-9.
26. Zhu Z.W., Zheng Q.R. (2016) Methane adsorption on the grapheme sheets, activated carbon and carbon black. *Appl. Therm. Eng.,* **108**, 605-13.
27. Mahmoudian L., Rashidi A., Dehgani H., Ranighi R. (2016) Single-step scalable synthesis of three-dimensional highly porous grapheme with favourable methane adsorption. *Chem. Eng. J.,* **304**, 784-92.

ABBREVIATIONS

ACs	activated carbons
AED	adsorption energy distribution
ANG	adsorbed natural gas
APW	average pore width, nm
b	Sips isotherm parameter, $bar^{-1/n}$
CMC	carboxy-methyl-cellulose sodium salt
CNG	compressed natural gas
DOE	department of energy
DFT	density functional theory
F(U)	adsorption energy distribution function
LNG	liquefied natural gas
m	mass of adsorbent, g
M	molar weight, g/mol
MRA	Mongolian raw anthracite
n	exponent of Sips equation
N	number of data
NG	natural gas
P	pressure, MPa
P_0	saturation pressure, MPa
P_{comp}	compression pressure, MPa
PMAC	potassium physical mixed activated carbon
PSD	pore size distribution
q_m	monolayer adsorption capacity, mmol/g
q^{cal}	calculated adsorption amount, mmol/g
q^{exp}	experimental adsorption amount, mmol/g
Q	gravimetric adsorption amount, mmol/g
R	universal gas constant, m^3• bar/K• mol
R_A	mass ratio of activating agent/anthracite
S_{BET}	BET surface area, m^2/g
SDP	successive destruction of pores
SOR	square of residual
U	adsorption energy, kJ/mol
v	volume occupied by 1 g of methane at STP, dm^3/g
V	volume of adsorption and loading cells, m^3
V_{BJH}	mesopore volume based on the BJH method, cm^3/g
V_{DFT}	micropore volume based on the DFT theory, cm^3/g
V_{HK}	micropore volume based on the HK method, cm^3/g
V_{sum}	sum of the HK and BJH pore volume, cm^3/g
V_t	total pore volume, cm^3/g
Z	compressibility factor
θ(P)	sub-monolayer surface coverage
ρ_{pack}	packing density, g/cm^3